Predicting High Harmonic Ion Cyclotron Heating Efficiency in Tokamak Plasmas

D. L. Green,* L. A. Berry, G. Chen, P. M. Ryan, and J. M. Canik
Oak Ridge National Laboratory, Post Office Box 2008, Oak Ridge, Tennessee 37831-6169, USA

E. F. Jaeger
XCEL Engineering Inc., 1066 Commerce Park Drive, Oak Ridge, Tennessee 37830, USA
(Received 16 March 2011; published 26 September 2011)

Observations of improved radio frequency (rf) heating efficiency in ITER relevant high-confinement (*H*-)mode plasmas on the National Spherical Tokamak Experiment are investigated by whole-device linear simulation. The steady-state rf electric field is calculated for various antenna spectra and the results examined for characteristics that correlate with observations of improved or reduced rf heating efficiency. We find that launching toroidal wave numbers that give fast-wave propagation in the scrape-off plasma excites large amplitude ($\sim$ kV m^{-1}) coaxial standing modes between the confined plasma density pedestal and conducting vessel wall. Qualitative comparison with measurements of the stored plasma energy suggests that these modes are a probable cause of degraded heating efficiency.

DOI: 10.1103/PhysRevLett.107.145001 PACS numbers: 52.50.Qt, 52.35.−g, 52.55.Fa, 52.65.−y

Introduction.—Our understanding of magnetically confined nuclear fusion has progressed to a state where net energy production is within reach. The next step towards achieving this goal is ITER [1], a reactor scale Tokamak currently under construction in Cadarache, France. To achieve fusion, ITER's plasma will be heated to $\sim$20 keV using 50 MW of external heating power from combined neutral beam injection (NBI) and both electron- and ion-cyclotron (IC) frequency rf waves. The rf waves are also used to drive current in order to control the background magnetic field and noninductively sustain the plasma. In this Letter we show that rf power in the IC frequency regime can excite normal modes of the plasma edge, whose presence correlates with decreased heating efficiency. This investigation is enabled by advances to the state-of-the-art in predictive computer simulation of IC heating and current drive for Tokamak plasmas relevant to ITER. Specifically, we use the first simulation to solve for the linear rf wave fields in a realistic whole-device configuration while maintaining all required kinetic physics for ITER relevant heating scenarios. We solve self-consistently for wave fields in both the well-confined core plasma and poorly confined scrape-off plasma (see Fig. 2). An ability to predict efficiency and performance of IC heating on ITER, and thus optimize heating scenarios, will be essential to the development of an economically viable magnetic confinement fusion power source. Such an ability will require high fidelity whole-device simulation with the work presented here being a step toward that goal. In addition, this work is relevant to general plasma wave propagation regimes where kinetic effects and strong density gradients across a boundary of open and closed magnetic field lines are important, e.g., kinetic Alfvén waves at Earth's magnetopause [2]. Significant progress in predicting the plasma response to ion-cyclotron radio-frequency (ICRF) waves in Tokamak plasmas has been achieved [3–5], largely coupled to the availability of leadership class computing facilities such as the Jaguar machine at the National Center for Computational Sciences. ITER D-T scenarios will be fast-wave heated at the first harmonic of deuterium and second of tritium. While high-harmonic fast-wave (HHFW) heating is used on the National Spherical Tokamak Experiment (NSTX) [6], for the present investigation of coupling fast-wave power from the antenna to the core plasma, NSTX provides a suitable test bed. Here we compare results from the whole-device [two-dimensional (2D) and three-dimensional (3D), antenna-to-core] simulation with recent experimental observations of improved IC heating efficiency on NSTX for a NBI *H*-mode scenario.

The NSTX IC antenna consists of a 12 strap phased array which toroidally spans $\sim$90° (see Fig. 3) and is capable of launching 6 MW of electromagnetic fast-wave power at 30 MHz. The fast-wave is typically strongly damped on electrons in a single pass through the core plasma via transit time magnetic pumping and electron Landau damping [7]. Using six decoupled power sources gives good control over the toroidal wave number (k_ϕ) of the launched wave. Experimental observations on NSTX show poor heating efficiency for small k_ϕ in both *L*- [8] and *H*-mode [9] scenarios. Heating efficiency was determined in these experiments by the correlation between launched rf power and measured increase in plasma stored energy for electrons (W_e) using a Thomson scattering diagnostic for kinetic electron pressure (cf. Fig. 2 of Ref. [8]). Since small k_ϕ waves are desired for their current drive efficiency characteristics [10], understanding why rf heating efficiency is poor for small k_ϕ is of importance. The dependence of heating efficiency on the launched k_ϕ has been interpreted by Refs. [8,11] in terms of the location

where the fast-wave transitions from evanescent in the antenna near-field to a propagating wave, i.e., the cutoff or onset location for fast-wave propagation. For scenarios with improved heating efficiency, the hypothesis is that this location is inside the core plasma (high temperature and pressure) defined by closed magnetic flux surfaces (cf. Fig. 2). Poor efficiency heating scenarios are expected to have the onset location in the scrape-off plasma (low temperature and pressure) that exists on open magnetic field lines near the wall and encompasses the antenna. This is explained using a zero-dimensional dispersion relation analysis where, given the confining magnetic field strength (B) and launched toroidal wave number, the onset density for fast-wave propagation is shown to be approximately proportional to Bk_ϕ^2/ω where ω is the angular rf frequency. Because of the $\frac{1}{R}$ falloff in toroidal magnetic field strength with radius (R) from the device center stack (cf. Fig. 3), launching a larger k_ϕ or increasing B effectively pushes the onset location away from the antenna and further into the plasma. It is suggested by Refs. [8,11] that fast-wave propagation in the scrape-off plasma can cause decreased rf heating efficiency due to possible formation of coaxial modes and damping of these edge waves via sheath effects or collisions in the low temperature plasma.

By retaining all relevant kinetic effects for the hot core plasma, including realistic density and temperature gradients between the core and scrape-off plasmas, and solving for the wave field out to the limiting vacuum vessel structures, we show that fast-wave propagation in the edge plasma is a plausible explanation for the observed degradation in rf heating efficiency. The following full-wave analysis reveals rf excited normal modes. These modes are not seen in linear plasma wave dispersion relation or ray tracing approaches.

Simulation details.—The simulation of rf wave propagation in hot plasmas is complicated by a nonlocal plasma response. Assuming a linear medium where the wave energy is much less than the plasma stored energy, the problem is typically Fourier transformed in space and time to a frequency domain Helmholtz wave equation containing a hot plasma dielectric tensor [12] that, due to the spatial nonlocality, has a dependence on wave number. Furthermore, in the magnetized plasmas considered here, the medium is highly anisotropic. As such, the dielectric is separated into directions parallel ($\parallel$) and perpendicular ($\perp$) to the confining magnetic field. However, the inclusion of a scrape-off plasma requires solving the Helmholtz system across the boundary between closed and open magnetic field lines (separatrix, cf. Fig. 2). Most hot plasma simulations use magnetic flux surface coordinates which break down at the separatrix. For this reason we utilize a spectral representation in all spatial directions via the all orders spectral algorithm (AORSA) [3]. AORSA uses Cartesian coordinates such that the directions for the spectral decomposition of the $\vec{\nabla}\times\vec{\nabla}\times$ piece of the Helmholtz equation are chosen independently of the background magnetic field. Therefore, the boundary between open and closed magnetic field lines is not significant in AORSA and the addition of a scrape-off plasma is straightforward, although limited as will be discussed. Also, for the NSTX HHFW heating scenarios considered in this Letter, the ion Larmor radius (ρ_i) can exceed the perpendicular wavelength ($k_\perp \rho_i \geq 1$) and the ion-cyclotron harmonic number (l) can be as high as 18. Being spectral (nonlocal) in all directions, AORSA ensures these physics are included. Such an approach produces a large dense matrix that requires leadership class computing facilities to factor and invert. The 3D simulation presented here required ~20 k processor hours with each 2D mode producing a matrix of ~1 TB.

While extending AORSA to include a scrape-off plasma avoids boundary condition matching problems associated with coupling a dedicated scrape-off plasma code to a core plasma code, it does come at a high computational cost that limits the scrape-off plasma resolution. This restricts us to qualitative comparison with experiment. The low resolution limitation is primarily due to the uniform spatial grid used by AORSA. At present there is no variable grid formulation of the Fourier spectral method compatible with the hot plasma dielectric tensor, and as such we cannot yet resolve the fine scale (mm) features of the antenna and Faraday shield.

Figure 1 shows the background density and temperature profiles used for the simulation. These were constructed to best match available experimental data from NSTX shot 130608 presented in Ref. [9]. This shot heats a NBI deuterium plasma with 1.8 MW of ICRF power. The equilibrium magnetic field is from an EFIT [13] reconstruction with a plasma current of 0.99 MA (0.54 T on axis toroidal

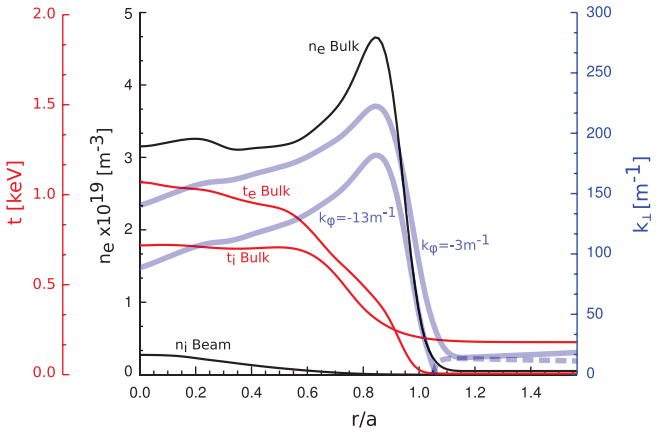

FIG. 1 (color). Midplane profiles for NSTX shot 130608 as used in the simulations presented here. Electron density (n_e) and temperature (T_e) are from multipoint Thomson scattering data, ion temperature (T_i) is from charge exchange recombination spectroscopy data, and the NBI fast-ion density (n_i) is from TRANSP [16] simulation. $a = 1.52$ m is the minor radius.

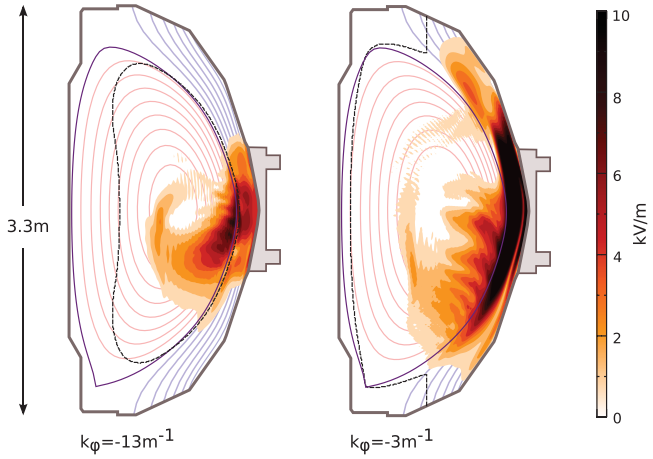

FIG. 2 (color). Two-dimensional AORSA simulation results of the steady-state wave electric field amplitude for HHFW on NSTX. The dashed line shows an approximate fast-wave cutoff based on a zero-dimensional dispersion calculation using $k_{\|} \approx k_{\phi} = n_{\phi}/R$. The separatrix is shown in purple, closed magnetic flux surfaces of the core plasma are in red, and open flux surfaces of the scrape-off plasma are in blue.

magnetic field strength). This is a H-mode shot where the density and temperature profiles exhibit a steep density gradient near the last closed magnetic flux surface (LCFS). One-dimensional midplane electron density (n_e) profiles are measured with Thompson scattering in the core and with microwave reflectometry in the scrape-off plasma. These data are mapped along closed flux surfaces to give 2D profiles for the core plasma. For estimating the 2D scrape-off n_e profile experimental midplane data near the LCFS are fit giving a decay of the form $n_e(\delta r) = 0.039 + 3.6\exp(-147.0\delta r^{1.4}) \times 10^{19}$ m^{-3} where δr is distance from the LCFS. This approach gives profiles that decay to a constant $n_e = 3.9 \times 10^{17}$ m^{-3} within a few cm of the LCFS. In addition, this minimum value of n_e in the scrape-off plasma is above that required for propagation of the short wavelength slow-wave mode [12]. As stated above, resolving such short wavelength modes will require improvements to AORSA. A similar procedure is followed for the bulk temperatures and NBI fast-ion density with the profiles shown in Fig. 1. The NBI fast-ion temperature profile is set to a flat 20 keV.

Simulation results.—Figure 2 shows 2D AORSA results for single toroidal modes $n_{\phi} = -22$, and -5 ($k_{\phi} = -13$ m^{-1}, -3 m^{-1}) corresponding to the dominant mode of the antenna spectrum for $\pm 180°$ and $-30°$ phasing, respectively. A clear dependence on the launched toroidal wave number can be seen. For large k_{ϕ} (-13 m^{-1}) the fast-wave is seen to be evanescent in the scrape-off plasma and begins to propagate at the core plasma where the density reaches the onset value (dashed line in Fig. 2). The wave is seen to penetrate the core plasma and is

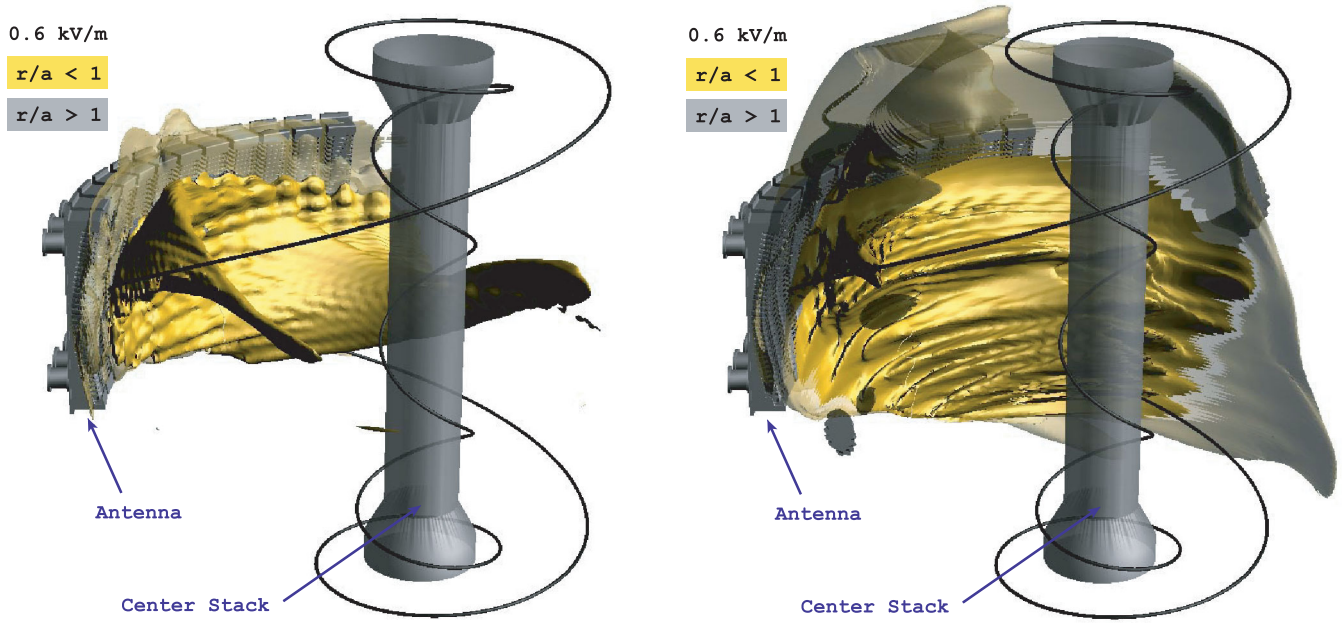

(a) $\pm 180°$ antenna phasing, dominant mode $k_{\phi} = \pm 13$ m^{-1}.

(b) $-30°$ antenna phasing, dominant mode $k_{\phi} = -3$ m^{-1}.

FIG. 3 (color). Three-dimensional AORSA results for the steady-state wave electric field amplitude. The gold (solid) and gray (transparent) contours are 0.6 kV m^{-1} and are inside and outside the LCFS, respectively. The antenna, center stack, and sample magnetic field line trajectory are shown. Figures were created using VISIT [14].

refracted back towards the low-field side before being absorbed primarily on electrons (56.5%) and NBI fast ions (36.1%). For small k_ϕ ($-3\ \mathrm{m}^{-1}$), there are large amplitude electric wave fields between the core plasma density gradient near the last closed magnetic flux surface and the antenna or vessel wall. The field magnitude plot shows a null indicating a standing coaxial mode as predicted by Ref. [8].

Figure 3 shows the $0.6\ \mathrm{kV\,m}^{-1}$ contour of the 3D electric wave field magnitude as calculated from the sum over $-50 \leq n_\phi \leq 50$ with toroidal mode spectral weightings calculated for antenna phasings of $\pm 180°$ and $-30°$. Figure 3(a) shows little fast-wave presence in the scrape-off plasma, and significant penetration of the core plasma. Figure 3(b) shows considerable fast-wave in the scrape-off plasma and poor core penetration.

Summary and conclusions.—The first whole-device 3D HHFW simulation to include realistic edge density profiles for a H-mode plasma, while retaining all orders in $k_\perp \rho_i$ and harmonic number, is presented. In addition to the typical fast-wave damping on electrons and NBI fast ions in the core plasma is a standing coaxial mode in the scrape-off plasma seen to be excited to large amplitude. Assuming the large amplitude coaxial mode is damped on collisions or nonlinear phenomena [15] (parasitic loss of power that would otherwise end up in the core plasma), we see qualitative agreement between simulation and experiment that supports the hypothesis that excitation of coaxial edge modes reduces ICRF heating efficiency.

The conclusions of this work have implications for ITER, where the separatrix-wall distance is large (10 to 20 cm). It may prove difficult to control the edge density in such a large region to below that for fast-wave propagation. Assuming an electron density at the separatrix in ITER of $n_0 = 1 \times 10^{19}\ \mathrm{m}^{-3}$, with a decay in the scrape-off plasma of the form $n(\delta r) = n_0 \exp(-\delta r / l_{\mathrm{SOL}})$ where δr is the distance from the LCFS and $l_{\mathrm{SOL}} = 4$ cm is the scrape-off plasma decay length, the onset location for fast-wave propagation for the dominant mode for $-90°$ antenna phasing ($n_\phi = -32$, $k_\phi = -3.84\ \mathrm{m}^{-1}$) is 11 cm from the wall, well within the scrape-off plasma. Therefore, optimizing the scrape-off plasma density profile will be important for ICRF heating efficiency on ITER.

Future work will focus on quantitative comparison of the scrape-off plasma electric field magnitudes with direct experimental observation and further improving predictive capability for ITER. This will require improving the resolution in the scrape-off plasma to resolve the antenna and Faraday shield. Also, the linear wave amplitude in the scrape-off plasma will be provided as invaluable input data to nonlinear simulations.

The authors wish to thank Benoit P. LeBlanc for providing TRANSP NBI profile data. This research used resources of the Oak Ridge Leadership Computing Facility, located in the National Center for Computational Sciences at Oak Ridge National Laboratory, and the National Energy Research Scientific Computing Center supported by the Office of Science of the Department of Energy under Contracts No. DE-AC05-00OR22725 and No. DE-AC02-05CH11231, respectively.

*greendl1@ornl.gov

[1] N. Holtkamp, Fusion Eng. Des. **82**, 427 (2007).
[2] J. R. Johnson and C. Z. Cheng, Geophys. Res. Lett. **24**, 1423 (1997).
[3] E. F. Jaeger *et al.*, Phys. Rev. Lett. **90**, 195001 (2003).
[4] E. Jaeger, R. Harvey, L. Berry, J. Myra, R. Dumont, C. Phillips, D. Smithe, R. Barrett, D. Batchelor, P. Bonoli, M. Carter, E. D'azevedo, D. D'ppolito, R. Moore, and J. Wright, Nucl. Fusion **46**, S397 (2006).
[5] D. L. Green, E. F. Jaeger, and L. A. Berry (RF-SciDAC Team), J. Phys. Conf. Ser. **180**, 012 058 (2009).
[6] M. Ono *et al.* (NSTX Team), Nucl. Fusion **40**, 557 (2000).
[7] M. Ono, Phys. Plasmas **2**, 4075 (1995).
[8] J. Hosea *et al.* (NSTX Team), Phys. Plasmas **15**, 056 104 (2008).
[9] G. Taylor *et al.* (NSTX Team), Phys. Plasmas **17**, 056 114 (2010).
[10] M. Brambilla, *Kinetic Theory of Plasma Waves* (Oxford University Press, New York, 1998).
[11] C. Phillips *et al.* (NSTX Team), Nucl. Fusion **49**, 075 015 (2009).
[12] T. H. Stix, *Waves in Plasmas* (Springer-Verlag, New York, 1992).
[13] S. Sabbagh *et al.* (NSTX Team), Nucl. Fusion **41**, 1601 (2001).
[14] http://visit.llnl.gov/.
[15] D. A. D'Ippolito and J. R. Myra, Phys. Plasmas **13**, 102 508 (2006).
[16] R. Budny, M. Bell, A. Janos, D. Jassby, L. Johnson, D. Manseld, D. McCune, M. Redi, J. Schivell, G. Taylor, T. Terpstra, M. Zarnstor, and S. Zweben, Nucl. Fusion **35**, 1497 (1995).